Resonant destruction as a possible solution to the cosmological lithium problem

Nachiketa Chakraborty,[1] Brian D. Fields,[1] and Keith A. Olive[2]

[1]*Departments of Astronomy and of Physics, University of Illinois, Urbana, Illinois 61801, USA*

[2]*William I. Fine Theoretical Physics Institute, University of Minnesota, Minneapolis, Minnesota 55455, USA*

(Received 8 November 2010; revised manuscript received 3 February 2011; published 23 March 2011)

We explore a nuclear physics resolution to the discrepancy between the predicted standard big-bang nucleosynthesis (BBN) abundance of ^{7}Li and its observational determination in metal-poor stars. The theoretical ^{7}Li abundance is 3–4 times greater than the observational values, assuming the baryon-to-photon ratio, $\eta_{\rm wmap}$, determined by WMAP. The ^{7}Li problem could be resolved within the standard BBN picture if additional destruction of $A = 7$ isotopes occurs due to new nuclear reaction channels or upward corrections to existing channels. This could be achieved via missed resonant nuclear reactions, which is the possibility we consider here. We find some potential candidate resonances which can solve the lithium problem and specify their required resonant energies and widths. For example, a 1^- or 2^- excited state of ^{10}C sitting at approximately 15.0 MeV above its ground state with an effective width of order 10 keV could resolve the ^{7}Li problem; the existence of this excited state needs experimental verification. Other examples using known states include $^7\mathrm{Be} + t \rightarrow {}^{10}\mathrm{B}(18.80\ \mathrm{MeV})$, and $^7\mathrm{Be} + d \rightarrow {}^{9}\mathrm{B}(16.71\ \mathrm{MeV})$. For all of these states, a large channel radius ($a > 10$ fm) is needed to give sufficiently large widths. Experimental determination of these reaction strengths is needed to rule out or confirm these nuclear physics solutions to the lithium problem.

DOI: 10.1103/PhysRevD.83.063006 PACS numbers: 26.35.+c

I. INTRODUCTION

Primordial nucleosynthesis continues to stand as our earliest probe of the universe based on standard model physics. Accurate estimates of the primordial abundances of the light elements D, ^{4}He and ^{7}Li within standard big-bang nucleosynthesis (BBN) [1–5] are crucial for making comparisons with observational determinations and ultimately testing the theory. Primordial abundances are also a probe of the early universe physics [6]. Currently, the theoretical estimates of D and ^{4}He match the observational values within theoretical and observational uncertainties [3,5] at the baryon-to-photon ratio determined by the 7-year WMAP data, $\eta_{\rm wmap} = 6.19 \pm 0.15 \times 10^{-10}$ [7]. In contrast, the theoretical primordial abundance of ^{7}Li does not match the observations.

At $\eta_{\rm wmap}$, the predicted BBN abundance of ^{7}Li is[1] [5]

$$\left(\frac{^7\mathrm{Li}}{\mathrm{H}}\right)_{\rm BBN} = (5.12^{+0.71}_{-0.62}) \times 10^{-10}. \quad (1)$$

The observed ^{7}Li abundance is derived from observations of low-metallicity halo dwarf stars which show a plateau [8] in (elemental) lithium versus metallicity, with a small scatter consistent with observational uncertainties. An analysis [9] of field halo stars gives a plateau abundance of

$$\left(\frac{\mathrm{Li}}{\mathrm{H}}\right)_{\rm halo\star} = (1.23^{+0.34}_{-0.16}) \times 10^{-10}. \quad (2)$$

However, the lithium abundance in several globular clusters tends to be somewhat higher [10,11], and a recent result found in [11] gave $^7\mathrm{Li/H} = (2.34 \pm 0.05) \times 10^{-10}$. Thus the theoretically estimated abundance of the isobar with mass 7 (^{7}Be + ^{7}Li) is more than the observationally determined value by a factor of 2.2–4.2 [5], at $\eta_{\rm wmap}$. Relative to the theoretical and observational uncertainties, this represents a deviation of 4.5–5.5σ.

This significant discrepancy constitutes the ''lithium problem'' which could point to limitations in either the observations, our theoretical understanding of nucleosynthesis, or the post-BBN processing of lithium.

On the theoretical front, strategies which have emerged to approach the lithium problem broadly either address astrophysics or microphysics. On the astrophysical side, one might attempt to improve our understanding of lithium depletion mechanisms operative in stellar models [12]. This remains an important goal but is not our focus here.

The microphysical solutions to the lithium problem all in some way change the nuclear reactions for lithium production in order to reduce the primordial (or pre-Galactic) lithium abundance to observed levels. Some of these work within the standard model, focusing on nuclear physics, in particular, the nuclear reactions involved in lithium production. One approach is to attempt to utilize the experimental uncertainties in the rates [2,13–15]. A second, related approach is the inclusion of new effects in the nuclear reaction database such as poorly understood resonance effects [16]. Finally, it may happen that effects beyond the standard model are responsible for the observed lithium abundance. For example, the primordial lithium abundance can be reduced by cosmological variation of the

[1]Note that the ^{7}Li abundance reported here differs slightly from that given in [5], primarily due to the small shift in η as reported in [7].

fine structure constant associated with a variation in the deuterium binding energy [17], or by the post-BBN destruction of lithium through the late decays of a massive particle in the early universe [18].

In this paper, we remain within the standard model, examining the possible role of resonant reactions which may have been up to now neglected. The requisite reduction in the ^{7}Li abundance can be achieved by either an enhancement in the rate of destruction of ^{7}Li or its mirror nucleus ^{7}Be. This approach is more promising than the alternative of reducing the production of ^{7}Be and ^{7}Li, where the reactions are better understood experimentally and theoretically [19–21], whereas the experimental and especially the theoretical situation for $A = 8$–11 has made large strides but still allows for surprises at the levels of interest to us [22].

The use of resonant channels is an approach that has paid off in the past in the context of stellar nucleosynthesis. Fred Hoyle famously predicted a resonant energy level at 7.68 MeV in the ^{12}C compound nucleus which enhances the $^8\mathrm{Be} + \alpha \rightarrow {}^{12}\mathrm{C}$ reaction cross section and allows the triple alpha reaction to proceed at relatively low densities [23]. Recently, it was shown that there are promising resonant destruction mechanisms which can achieve the desired reduction of the total $A = 7$ isotopic abundance [16]. This paper points to a resonant energy level at $(E, J^\pi) = (16.71\ \mathrm{MeV}, 5/2^+)$ in the ^{9}B compound nucleus which can increase the rate of the $^7\mathrm{Be}(d, p)\alpha\alpha$ and/or $^7\mathrm{Be}(d, \gamma)^9\mathrm{B}$ and thereby reduce the ^{7}Be abundance. Here, we take a more general approach and systematically search for all possible compound nuclei [24] and potential resonant channels which may result in the destruction of ^{7}Be and/or ^{7}Li.

Because of the large discrepancy between the observed and BBN abundance of ^{7}Li, any nuclear solution to the lithium problem will require a significant modification to the existing rates. As we discuss in the semianalytic estimate in Sec. II, any new rate or modification to an existing one, must be 2–3 times greater than the current dominant destruction channels, namely, $^7\mathrm{Li}(p, \alpha)\alpha$ for ^{7}Li and $^7\mathrm{Be}(n, p)^7\mathrm{Li}$ for ^{7}Be. As discussed in [15] and as we show semianalytically in Sec. II, this is difficult to achieve with nonresonant reactions. Hence, we will concentrate on possible resonant reactions as potential solutions to the lithium problem. As we will show, there are interesting candidate resonant channels which may resolve the ^{7}Li problem. For example, there is a possibility of destroying ^{7}Be through a 1^- or 2^- ^{10}C excited state at approximately 15.0 MeV. The energy range between 6.5 and 16.5 MeV is currently very poorly mapped out and a state near the entrance energy for $^7\mathrm{Be} + {}^3\mathrm{He}$ could provide a solution if the effective width is of order 10 keV. We will also see that these reactions all require fortuitously favorable nuclear parameters, in the form of large channel radii, as also found by Cyburt and Pospelov [16] in the case of $^7\mathrm{Be} + d$. Even so, in the face of the more radical alternative of new fundamental particle physics, these more conventional solutions to the lithium problem beckon for experimental testing.

The paper is organized as follows: First, we lay down the required range of properties of any resonance to solve the lithium problem by means of a semianalytic estimate inspired by [25,26] in Sec. II. Then, in Sec. III, we list experimentally identified resonances from the databases: TUNL [24] and NNDC [27], involving either the destruction of ^{7}Be or ^{7}Li. Finally, the solution space of resonant properties, wherein the lithium problem is partially or completely solved, is mapped for the most promising initial states involving either ^{7}Li or ^{7}Be, by including these rates in a numerical estimation of the ^{7}Li abundance. This exercise will delineate the effectiveness of experimentally studied or identified resonances as well as requirements of possible missed resonant energy levels in compound nuclei formed by these initial states. This is described in Sec. IV. We note that in our analysis, the narrow resonance approximation is assumed which may not hold true in certain regions of this solution space. Our key results are pared down to a few resonant reactions described in Sec. V. A summary and conclusions are given in Sec. VI.

II. SEMIANALYTIC ESTIMATE OF IMPORTANT REACTION RATES

Before we embark on a systemic survey of possible resonant enhancements of the destruction of $A = 7$ isotopes, it will be useful to estimate the degree to which the destruction rates must change in order to have an impact on the final ^{7}Li abundance. The net rate of production of a nuclide i is given by the difference between the production from nuclides k and l and the destruction rates via nuclide j, i.e., for the reaction $i + j \rightarrow k + l$. This is expressed quantitatively by the rate equation [28] for abundance change

$$\frac{dn_i}{dt} = -3Hn_i + \sum_{jkl} n_k n_l \langle \sigma v \rangle_{kl} - n_i n_j \langle \sigma v \rangle_{ij}, \qquad (3)$$

where n_i is the number density of nuclide i, H is the Hubble parameter, $\sum_{ij} n_i n_j \langle \sigma v \rangle_{ij}$ are the sum of contributions from all the forward reactions destroying nuclide i, and $\sum_{kl} n_k n_l \langle \sigma v \rangle_{kl}$ are the reverse reactions producing it. $\langle \sigma v \rangle$ is the thermally averaged cross section of the reaction. The dilution of the density of these nuclides due to the expansion of the universe can be removed by reexpressing Eq. (3) in terms of number densities relative to the baryon density $Y_i \equiv n_i/n_b$, as

$$\frac{dY_i}{dt} = n_b \sum_{jkl} Y_k Y_l \langle \sigma v \rangle_{kl} - Y_i Y_j \langle \sigma v \rangle_{ij}. \qquad (4)$$

Using this general form, the net rate of ^{7}Be production can be approximated in terms of the thermally averaged cross sections of its most important production and destruction channels as

$$\frac{dY_{^7\mathrm{Be}}}{dt} = n_b(\langle\sigma v\rangle_{^3\mathrm{He}\alpha} Y_{^3\mathrm{He}} Y_\alpha - \langle\sigma v\rangle_{^7\mathrm{Be}n} Y_{^7\mathrm{Be}} Y_n). \quad (5)$$

Here, the reverse reaction rates of these production and destruction channels are neglected, as they are much smaller than the forward rates at the lithium synthesis temperature. A similar equation can be written down for ^{7}Li. When quasistatic equilibrium is reached, the destruction and production rates are equal. In this case, approximate values for new rates, which can effectively destroy either isobar, can be obtained analytically.

At temperatures $T \approx 0.04$ MeV, both ^{7}Li and ^{7}Be are in equilibrium [26] which gives

$$\langle\sigma v\rangle_{^3\mathrm{He}\alpha} Y_{^3\mathrm{He}} Y_\alpha = \langle\sigma v\rangle_{^7\mathrm{Be}n} Y_{^7\mathrm{Be}} Y_n. \quad (6)$$

Consider a new, inelastic ^{7}Be destruction channel $^7\mathrm{Be} + X \to Y + Z$, involving projectile X. This reaction will add to the right-hand side of Eq. (6) and shift the equilibrium abundance of ^{7}Be to a new value as follows:

$$Y^{\mathrm{new}}_{^7\mathrm{Be}} \approx \frac{\langle\sigma v\rangle_{^3\mathrm{He}\alpha} Y_\alpha Y_{^3\mathrm{He}}}{\langle\sigma v\rangle_{^7\mathrm{Be}n} Y_n + \langle\sigma v\rangle_{^7\mathrm{Be}X} Y_X} \approx \frac{1}{1 + \frac{\langle\sigma v\rangle_{^7\mathrm{Be}X} Y_X}{\langle\sigma v\rangle_{^7\mathrm{Be}n} Y_n}} Y^{\mathrm{old}}_{^7\mathrm{Be}}. \quad (7)$$

If the new reaction is to be important in solving the lithium problem, it must reduce the ^{7}Be abundance by a factor of $Y^{\mathrm{new}}_{^7\mathrm{Be}}/Y^{\mathrm{old}}_{^7\mathrm{Be}} \sim 3$–$4$. This in turn demands via Eq. (7) that $\langle\sigma v\rangle_{^7\mathrm{Be}X} Y_X/\langle\sigma v\rangle_{^7\mathrm{Be}n} Y_n \sim 2$–$3$, i.e., the rate for the new reaction exceeds that of the usual n-p interconversion reaction rate. A similar estimate can be made for ^{7}Li.

This reasoning would exclude nonresonant rates as they would be required to have unphysically large astrophysical S factors in the range of order 10^5–10^9 keV-barn depending on the channel. Thus we would expect that only resonant reactions can produce the requisite high rates. Possible resonant reactions are listed in the next section, whose key properties of resonance strength Γ_{eff} and energy E_{res} lie in appropriate ranges capable of achieving the required destruction of mass 7.

Finally, we turn to ^{7}Li destruction reactions, $^7\mathrm{Li} + X \to Y + Z$. Recall that at the WMAP value of η, mass 7 is made predominantly as ^{7}Be, with direct ^{7}Li production about an order of magnitude smaller. This suggests that enhancing direct ^{7}Li destruction will only modestly affect the final mass-7 abundance; we will see that this expectation is largely correct.[2]

[2]A subtle point is that normally, the mass-7 abundance is most sensitive to rate $^7\mathrm{Be}(n, p)^7\mathrm{Li}$ [29]. Of course, this reaction leaves the mass-7 abundance unchanged, but the lower Coulomb barrier for ^{7}Li leaves it vulnerable to the $^7\mathrm{Li}(p, \alpha)^4\mathrm{He}$ reaction, which is extremely effective in removing ^{7}Li. Thus, for a new, resonant ^{7}Li destruction reaction to be important, it must successfully compete with the very large $^7\mathrm{Li}(p, \alpha)^4\mathrm{He}$ rate, and even then the mass-7 destruction "bottleneck" remains the $^7\mathrm{Be}(n, p)^7\mathrm{Li}$ rate that limits ^{7}Li appearance. Thus we would not expect direct ^{7}Li destruction to be effective. We will examine ^{7}Li destruction below, and confirm these expectations.

With these pointers, the list in the next section is reduced and numerical analysis of the remaining promising rates is done.

III. SYSTEMATIC SEARCH FOR RESONANCES

In this section we describe a systematic search for nuclear resonances which could affect primordial lithium production. We first begin with general considerations, then catalog the candidate resonances. We briefly review the basic physics of resonant reactions to establish notation and highlight the key physical ingredients.

A. General considerations

Energetically, the net process $^7\mathrm{Be} + A \to B + D$ must have $Q + E_{\mathrm{init}} \geq 0$, where the initial kinetic energy $E_{\mathrm{init}} \simeq T \lesssim 40$ keV is small at the epoch of $A = 7$ formation. Thus we in practice require exothermic reactions, $Q > 0$. Moreover, inelastic reactions with large Q will yield final-state particles with large kinetic energies. Such final states thus have larger phase space than those with small Q and in that sense should be favored.

Consider now a process $^7\mathrm{Be} + X \to C^* \to Y + Z$ which destroys ^{7}Be via a resonant compound state; a similar expression can be written for ^{7}Li destruction. In the entrance channel $^7\mathrm{Be} + X \to C^*$ the energy released in producing the compound state is $Q_C = \Delta(^7\mathrm{Be}) + \Delta(X) - \Delta(C^{\mathrm{g.s.}})$, where $\Delta(A) = m - Am_{\mathrm{u}}$ is the mass defect. If an excited state C^* in the compound nucleus lies at energy E_{ex}, then the difference

$$E_{\mathrm{res}} \equiv E_{\mathrm{ex}} - Q_C \quad (8)$$

determines the effectiveness of the resonance. We can expect resonant production of C^* if $E_{\mathrm{res}} \lesssim T$. In an ordinary ("superthreshold") resonance we then have $E_{\mathrm{res}} > 0$, while a subthreshold resonance has $E_{\mathrm{res}} < 0$.

Once formed, the excited C^* level can decay via some set of channels. The cross section for $^7\mathrm{Be} + X \to C^* \to Y + Z$ is given by the Breit-Wigner expression

$$\sigma(E) = \frac{\pi\omega}{2\mu E} \frac{\Gamma_{\mathrm{init}}\Gamma_{\mathrm{fin}}}{(E - E_{\mathrm{res}})^2 + (\Gamma_{\mathrm{tot}}/2)^2}, \quad (9)$$

where E is the center-of-mass kinetic energy in the initial state, μ is the reduced mass, and

$$\omega = \frac{2J_{C^*} + 1}{(2J_X + 1)(2J_7 + 1)} \quad (10)$$

is a statistical factor accounting for angular momentum. The width of the initial state (entrance channel) is Γ_{init}, and the width of the final state (exit channel) is Γ_{fin}.

One decay channel which must always be available is the entrance channel itself. Obviously such an elastic reaction is useless from our point of view. Rather, we are interested in inelastic reactions in which the initial ^{7}Be (or ^{7}Li) is transformed to something else. In some cases, an

inelastic strong decay is possible where the final-state particles $Y + Z$ are both nuclei. Note that it is possible to produce a final-state nucleus in an excited state, e.g., $C^* \to Y^* + Z$, in which case the energy release Q'_C is offset by the Y^* excitation energy. This possibility increases the chances of finding energetically allowable final states. Indeed, such a possibility has been suggested in connection with the $^7\mathrm{Be} + d \to {}^9\mathrm{B}^* \to {}^8\mathrm{Be}^* + p$ process [16].

Regardless of the availability of a strong inelastic channel, an electromagnetic transition $C^* \to C^{(*)} + \gamma$ to a lower level is always possible. However, these often have small widths and thus a small branching ratio $\Gamma_{\mathrm{fin}}/\Gamma_{\mathrm{tot}}$. Thus for electromagnetic decays to be important, a strong inelastic decay must not be available, and the rest of the reaction cross section needs to be large to compensate the small branching; as seen in Eq. (9), this implies that Γ_{init} be large.

Note that in all charged-particle reactions, the Coulomb barrier is crucially important and is implicitly encoded via the usual exponential Gamow factor in the reaction widths of both initial and final charged-particle states. However, if the reaction has a high Q, the final-state kinetic energy will be large and thus there will not be significant final-state Coulomb suppression; this again favors final states with large Q. In addition, if the entrance or exit channel has orbital angular momentum $L > 0$, there is additional exponential suppression, so that $L > 0$ states are disfavored for our purposes.

With these requirements in mind, we will systematically search for resonant reactions which could ameliorate or solve the lithium problem. We begin by identifying possible processes which are

(1) *new* resonances not yet included in the BBN code;
(2) 2-body to 2-body processes, since 3-body rates are generally very small in BBN due to phase space suppression as well as the relatively low particle densities and short time scales;
(3) experimentally allowed—in practice this means we seek unidentified states in poorly studied regimes;
(4) *narrow* resonances having $\Gamma_{\mathrm{tot}} \lesssim T$, which is around $\Gamma_{\mathrm{tot}} < 40$ keV but we will also consider somewhat larger widths to be conservatively generous;
(5) relatively low-lying resonances with $E_{\mathrm{res}} \lesssim$ few $\times$ $T \sim 100$–300 keV, which are thermally accessible; here again we err on the side of a generous range.

Once we have identified all possible candidate resonances, we will then assess their viability as solutions to the lithium problem based on available nuclear data.

B. List of candidate resonances

As described above, we will explore the resonant destruction channels of both ^{7}Li and ^{7}Be. Some of the potential resonances which might be able to reduce the mass 7 abundance to the observed value were recently considered in [16]. This analysis eliminates several candidate resonances, leaving as genuine solutions only the resonance related to the $^7\mathrm{Be}(d, \gamma)^9\mathrm{B}$ and $^7\mathrm{Be}(d, p)\alpha\alpha$ reactions and associated with the 16.71 MeV level in the ^{9}B compound nucleus. Here, we make an exhaustive list of possible promising resonances that may be important to either ^{7}Be or ^{7}Li destruction channels. In order to do so systematically and account for all possible resonances that may be of importance, we study the energy levels in all possible compound nuclei that may be formed in destroying ^{7}Be or ^{7}Li, making extensive use of databases at TUNL and the NNDC [24,27].

The available 2-body destruction channels $^7A + X$ may be classified by $X = n$, p, d, t, ^{3}He, α, and γ. Consequently, the compound nuclei that can be formed starting from mass 7 have mass numbers ranging from $A = 8$ to $A = 11$, and the ones of particular interest are ^{8}Li, ^{8}Be, ^{8}B, ^{9}Be, ^{9}B, ^{10}Be, ^{10}B, ^{10}C, ^{11}B, and ^{11}C. All relevant, resonant energy levels in these compound nuclei that may provide paths for reduction of mass-7 abundance are listed in Tables I, II, III, IV, V, VI, VII, VIII, IX, and X.

There are quantum mechanical and kinematic restrictions to our selection of candidates. The candidate resonant reactions must obey selection rules. The partial widths for a channel, which may be viewed as probability currents of emission of the particle in that channel through the nuclear surface, are given as

$$\Gamma_L(E) = 2kaP_L(E, a)\gamma^2(a), \tag{11}$$

where a is the channel radius and E is the projectile energy. Here k is the wave number of the colliding particles in the center-of-mass frame and γ^2 is the reduced width, which depends on the overlap between the wave functions inside and outside the nuclear surface, beyond which the nuclear forces are unimportant. The reduced width γ^2 is independent of energy and has a statistical upper limit called the Wigner limit given by [30]

$$\gamma^2 \leq \frac{3\hbar^2}{2\mu a^2}. \tag{12}$$

The prefactor of $\frac{3}{2}$ is under the assumption that the nucleus is uniform and can change to within a factor of order unity if this assumption changes. The Wigner limit depends sensitively on the channel radius and thus varies with the nuclei involved. For the nuclei of our interest, typical values of γ^2 range from a few hundred keV to a few MeV.

In Eq. (11), $P_L(E, a)$ is the Coulomb penetration probability for angular momentum L and is a strong and somewhat complicated function of E and a. Thus, while the Wigner limit sets a theoretical limit on the reduced width, the upper limit on the full width $\Gamma_L(E)$ depends on the values of $P_L(E, a)$ and is sensitive to the details of the resonant channel being considered. In light of this complexity, our strategy is as follows. We evaluate the $\Gamma_L(E)$ needed to make a substantial impact on the lithium problem. Then for the cases of highest interest, we will compare

TABLE I. This table lists the potential resonances in ^{8}Li, ^{8}Be, and ^{8}B which may achieve required destruction of mass 7. These are all allowed by selection rules and include some resonances already accounted for in determining the current theoretical ^{7}Li abundance indicated as (included). The entrance and exit channels along with their partial and total widths (Γ_{tot}), minimum angular momenta (L_{init}, L_{fin}), as well as resonance energies are listed wherever experimental data are available. The starred widths are a result of fits from R-matrix analysis. The list includes final products in ground and excited states with the latter marked with a star in the superscript.

Compound nucleus, J^π, E_{ex}	Initial state	L_{init}	L_{fin}	E_{res}	Γ_{tot}	Exit channels	Exit channel width
^{8}Li, 3^+, 2.255 MeV	^{7}Li + n	1	1	222.71 keV	33 ± 6 keV	γ (ground state)	$7.0 \pm 3.0 \times 10^{-2}$eV
(included)			1			n (elastic) ≈ 100%	33 ± 6 keV
^{8}Be, 2^+, 16.922 MeV	^{7}Li + p	1	2	−333.1 keV	74.0 ± 0.4 keV	γ (ground state)	$8.4 \pm 1.4 \times 10^{-2}$eV
			1			γ(3.04 MeV)	<2.80 ± 0.18 eV
			2			$\alpha \approx 100\%$	≈ 74.0 keV
			1			p (elastic)	unknown
^{8}Be, 1^+, 17.640 MeV	^{7}Li + p	1	1	384.9 keV	10.7 keV	γ (ground state)	16.7 eV
			1			γ(3.04 MeV)	6.7 ± 1.3 eV
			2			γ(3.04 MeV)	0.12 ± 0.05 eV
			1			γ(16.63 MeV)	$(3.2 \pm 0.3) \times 10^{-2}$ eV
			1			γ(16.92 MeV)	$(1.3 \pm 0.3) \times 10^{-3}$ eV
			1			p (elastic) 98.8%	10.57 keV
^{8}Be, 2^-, 18.91 MeV	^{7}Be + n	0	1	10.3 keV	122 keV*	γ(16.922 MeV)	$9.9 \pm 4.3 \times 10^{-2}$ eV
(included)			1			γ (16.626 MeV)	0.17 ± 0.07 eV
			0			p	<105.1 keV*
			2			p + ^{7}Li* (0.4776 MeV)	<105.1 keV*
			0			n (elastic)	16.65 keV*
^{8}Be, 3^+, 19.07 MeV	^{7}Be + n	1	1	170.3 keV	270 ± 20 keV	$p \approx 100\%$	<270 keV
(included)			3			p + ^{7}Li*(0.4776 MeV)	<270 keV
			1			γ(3.03 MeV)	10.5 eV
			1			n (elastic)	unknown
^{8}Be, 3^+, 19.235 MeV	^{7}Be + n	1	1	335.3 keV	227 ± 16 keV	$p \approx 50\%$	≈ 113.5 keV
(included)			1			γ(3.03 MeV)	10.5 eV
			1			n (elastic) ≈ 50%	≈ 113.5 keV
^{8}Be, 1^-, 19.40 MeV	^{7}Be + n	0	0	500.3 keV	645 keV	p	unknown
			0			p + ^{7}Li* (0.4776 MeV)	unknown
			0			n (elastic)	unknown
			1			α	unknown
^{8}B$^{g.s.}$, 2^+, 0 MeV	^{7}Be + p	1	1	−0.1375 MeV	unknown	p (elastic)	unknown
			0			EC → ^{8}Be	8.5×10^{-19} eV
^{8}B, 1^+, 0.7695 MeV	^{7}Be + p	1	1	630 ± 3 keV	35.7 ± 0.6 keV	γ (ground state)	25.2 ± 1.1 meV
(included)			1			p (elastic) 100%	35.7 ± 0.6 keV

our results with the theoretical limit set by the Coulomb suppressed Wigner limit for those specific cases.

We also limit our consideration to two body initial states, with resonance energies $E_{res} \leq 650$ keV. The high resonance energy limit ensures that all possible resonances which may influence the final ^{7}Li abundance are taken into account, though many of the channels with such high resonance energies will inevitably be eliminated. Excited final states have also been considered in making this list. Different excited states of final-state products are marked as separate entries in the table, since each one has its own spin and therefore a different angular momentum barrier. And thereby the significance of each excited state in destroying mass 7 is varied. Also, we usually eliminate the reactions with a negative Q-value except for the ^{7}Li(d, p)^{8}Li, ^{7}Be(d, ^{3}He)^{6}Li, ^{7}Be(d, p)^{8}Be* (16.922 MeV) and ^{7}Li(^{3}He, p)^{9}Be* (11.283 MeV) as they are only marginally endothermic.

For a number of the reactions listed in these tables I, II, III, IV, V, VI, VII, VIII, IX, and X, the total spin of the initial state reactants is equal to that of the compound nucleus, which is equal to the total spin of the products, with $L = 0$. However, for many reactions, angular momentum is required in the initial and/or final state, which decreases the penetration probability and thereby the width for that particular channel. In fact for some of these

TABLE II. As in Table I, listing the potential resonances in ^{9}Be.

Compound nucleus, J^π, E_{ex}	Initial state	L_{init}	L_{fin}	E_{res}	Γ_{tot}	Exit channels	Exit channel width
^{9}Be,	^{7}Li + d	1	unknown	−24.9 keV	41 ± 4 keV	γ	unknown
$(5/2^+)$, 16.671 MeV			2			$n + {}^8$Be	unknown
			0			$n + {}^8$Be* (3.03 MeV)	unknown
			2			$n + {}^8$Be* (11.35 MeV)	unknown
			0			p	unknown
			1			α	unknown
			1			d (elastic)	unknown
^{9}Be,	^{7}Li + d	0	1	279.3 keV	389 ± 10 eV	γ (ground state)	16.9 ± 1.0 eV
$1/2^-$, 16.9752 MeV			1			γ (1.68 MeV)	1.99 ± 0.15 eV
			2			γ (2.43 MeV)	0.56 ± 0.12 eV
			1			γ (2.78 MeV)	2.2 ± 0.7 eV
			unknown			γ (Unknown level, TUNL)	<0.8 eV
			1			γ (4.70 MeV)	2.2 ± 0.3 eV
			1			p	12^{+12}_{-6} eV
			1			n	<288 eV
			1			$n + {}^8$Be* (3.03 MeV)	<288 eV
			3			$n + {}^8$Be* (11.35 MeV)	<288 eV
			2			α	<241 eV
			0			d (elastic)	62 ± 10 eV
^{9}Be,	^{7}Li + d	0	unknown	602.1 keV	200 keV	γ (ground state)	unknown
$(5/2)^-$, 17.298 MeV			1			p	194.4 keV
(included)			3			$n + {}^8$Be	unknown
			1			$n + {}^8$Be* (3.03 MeV)	unknown
			1			$n + {}^8$Be* (11.35 MeV)	unknown
			2			α	unknown
			0			d (elastic)	unknown

reactions, parity conservation demands higher angular momentum which worsens this effect. However, we do not reject any channel based on the angular momentum suppression of its width in these tables. Later we will shortlist those resonant channels which are not very suppressed and indeed potentially effective in destroying mass 7.

The reactions of interest are listed in increasing order of the mass of the compound nuclei formed. The particular

TABLE III. As in Table I, listing the potential resonances in ^{9}B.

Compound nucleus, J^π, E_{ex}	Initial state	L_{init}	L_{fin}	E_{res}	Γ_{tot}	Exit channels	Exit channel width
^{9}B $(5/2^+)$, 16.71 MeV	^{7}Be + d	1	2	219.9 keV	unknown	$p + {}^8$Be	unknown
			0			$p + {}^8$Be* (3.03 MeV)	unknown
			2			$p + {}^8$Be* (11.35 MeV)	unknown
			0			$p + {}^8$Be* (16.626 MeV)	unknown
			0			$p + {}^8$Be* (16.922 MeV)	unknown
			2			^{3}He	unknown
			1			$\alpha + {}^5$Li	unknown
			3			$\alpha + {}^5$Li* (1.49 MeV)	unknown
			1			d (elastic)	unknown
^{9}B, $(1/2^-)$, 17.076 MeV	^{7}Be + d	0	1	585.9 keV	22 keV	$p + {}^8$Be	unknown
			1			$p + {}^8$Be* (3.03 MeV)	unknown
			3			$p + {}^8$Be* (11.35 MeV)	unknown
			1			$p + {}^8$Be* (16.626 MeV)	unknown
			1			^{3}He	unknown
			2			$\alpha + {}^5$Li	unknown
			0			$\alpha + {}^5$Li* (1.49 MeV)	unknown
			0			d (elastic)	unknown

TABLE IV. As in Table I, listing the potential resonant reactions in ^{10}Be.

Compound nucleus, J^π, E_{ex}	Initial state	L_{init}	L_{fin}	E_{res}	Γ_{tot}	Exit channels	Exit channel width
^{10}Be,	^{7}Li + t	0	0	−130.9 keV	≈ 150 keV	n + ^{9}Be	unknown
(2^-), 17.12 MeV			1			n + ^{9}Be* (1.684 MeV)	unknown
			0			n + ^{9}Be* (2.4294 MeV)	unknown
			2			n + ^{9}Be* (2.78 MeV)	unknown
			1			n + ^{9}Be* (3.049 MeV)	unknown
			1			n + ^{9}Be* (4.704 MeV)	unknown
			0			n + ^{9}Be* (5.59 MeV)	unknown
			2			n + ^{9}Be* (6.38 MeV)	unknown
			3			n + ^{9}Be* (6.76 MeV)	unknown
			0			n + ^{9}Be* (7.94 MeV)	unknown
			0			t (elastic)	unknown
^{10}Be,	^{7}Li + t	unknown	unknown	539.1 keV	112 ± 35 keV	γ	3 + 2 eV
unknown, 17.79 MeV			unknown			n + ^{9}Be	<77 keV
			unknown			n + ^{9}Be* (1.684 MeV)	<77 keV
			unknown			n + ^{9}Be* (2.4294 MeV)	<77 keV
			unknown			n + ^{9}Be* (2.78 MeV)	<77 keV
			unknown			n + ^{9}Be* (3.049 MeV)	<77 keV
			unknown			n + ^{9}Be* (4.704 MeV)	<77 keV
			unknown			n + ^{9}Be* (5.59 MeV)	<77 keV
			unknown			n + ^{9}Be* (6.38 MeV)	<77 keV
			unknown			n + ^{9}Be* (6.76 MeV)	<77 keV
			unknown			n + ^{9}Be* (7.94 MeV)	<77 keV
			unknown			t (elastic)	78 keV

resonant energy levels of interest E_{ex} and their spins are listed in the table. In general, different initial states involving ^{7}Li and ^{7}Be can form these energy levels and so all these relevant initial states are listed. For each one, the various final product states for an inelastic reaction are enumerated. Again, each of the final-state products can also be formed in an excited state. These excited states must have lower energy than the initial state energies for the reaction to be exothermic. In addition spin and parity must be conserved. Enforcing these, the minimum final-state angular momenta L_{fin} are evaluated from the spin of the resonant energy level and are listed in the tables. The total widths of the energy levels are listed whenever available. The partial widths of the different channels including the elastic one, out of each energy level are also listed.

We adopt the narrow resonance approximation to evaluate the effect of these resonances and either retain or dismiss them as potential solutions to the lithium problem. Some of the partial widths or limits on them are high enough that they easily qualify to be broad resonances. This implies that the narrow resonance formula used to see their effect is not precise, but still gives a rough idea of whether the resonance is ineffective or not.

Our expression for thermonuclear rates in the narrow resonance approximation is explained in detail in Appendix A, and is given by

$$\langle \sigma v \rangle = \omega \Gamma_{\rm eff} \left(\frac{2\pi}{\mu T} \right)^{3/2} e^{-|E_{\rm res}|/T} f(2E_{\rm res}/\Gamma_{\rm tot}). \quad (13)$$

This rate is controlled by two parameters specific to the compound nuclear state: E_{res} and Γ_{eff}. Here E_{res} is given in Eq. (8), and measures the offset from the entrance channel and the compound state. The resonance strength is quantified via

$$\Gamma_{\rm eff} = \frac{\Gamma_{\rm init}\Gamma_{\rm fin}}{\Gamma_{\rm tot}}, \quad (14)$$

with Γ_{init} and Γ_{fin} being the entrance and exit widths of a particular reaction, and Γ_{tot} the sum of the widths of all possible channels. Of these widths, the smaller of Γ_{init} and Γ_{fin} along with Γ_{tot} are listed in the tables. The resonance strength $\Gamma_{eff} \approx \Gamma_{init}$, if Γ_{fin} dominates the total width and vice versa. If Γ_{init} and Γ_{fin} are the dominant partial widths and they are comparable to each other, then the strength is even higher.

As discussed in Appendix A, our narrow resonance rate in Eq. (13) improves on the form of the usual expression for narrow resonance in two ways: (a) it extends to the subthresold domain; and (b) it introduces the factor f which accounts for a finite E_{res}/Γ_{tot} ratio.

It is important to make a systematic and comprehensive search for all possible experimentally identified resonances capable of removing this discrepancy. In addition, it is possible that resonances and indeed energy levels themselves were missed, especially at the higher energies, where uncertainties are greater. Therefore it is useful to map the parameter space, where the lithium discrepancy is removed, to *a priori* lay down our expectations of such

TABLE V. As in Table I, listing the ground and excited final states for the 18.2 MeV energy level in ^{10}B.

Compound nucleus, J^π, E_{ex}	Initial state	L_{init}	L_{fin}	E_{res}	Γ_{tot}	Exit channels	Exit channel width
^{10}B,	^{7}Li + ^{3}He	unknown	unknown	411.7 keV	1500 ± 300 keV	$p + {}^9$Be	unknown
unknown (18.2 MeV)			unknown			$p + {}^9$Be* (1.684 MeV)	unknown
			unknown			$p + {}^9$Be* (2.4294 MeV)	unknown
			unknown			$p + {}^9$Be* (2.78 MeV)	unknown
			unknown			$p + {}^9$Be* (3.049 MeV)	unknown
			unknown			$p + {}^9$Be* (4.704 MeV)	unknown
			unknown			$p + {}^9$Be* (5.59 MeV)	unknown
			unknown			$p + {}^9$Be* (6.38 MeV)	unknown
			unknown			$p + {}^9$Be* (6.76 MeV)	unknown
			unknown			$p + {}^9$Be* (7.94 MeV)	unknown
			unknown			$p + {}^9$Be* (11.283 MeV)	unknown
			unknown			$n + {}^9$B	unknown
			unknown			$n + {}^9$B* (1.6 MeV)	unknown
			unknown			$n + {}^9$B* (2.361 MeV)	unknown
			unknown			$n + {}^9$B* (2.75 MeV)	unknown
			unknown			$n + {}^9$B* (2.788 MeV)	unknown
			unknown			$n + {}^9$B* (4.3 MeV)	unknown
			unknown			$n + {}^9$B* (6.97 MeV)	unknown
			unknown			$d + {}^8$Be	unknown
			unknown			$d + {}^8$Be* (3.03 MeV)	unknown
			unknown			$d + {}^8$Be* (11.35 MeV)	unknown
			unknown			t	unknown
			unknown			$\alpha + {}^6$Li	unknown
			unknown			$\alpha + {}^6$Li* (2.186 MeV)	unknown
			unknown			$\alpha + {}^6$Li* (3.563 MeV)	unknown
			unknown			$\alpha + {}^6$Li* (4.31 MeV)	unknown
			unknown			$\alpha + {}^6$Li* (5.37 MeV)	unknown
			unknown			^{3}He (elastic)	unknown

missed resonances. This can be done by looking at interesting initial states involving ^{7}Li and ^{7}Be, and abundant projectiles p, n, d, t, ^{3}He, α, and parametrizing the effect of inelastic channels on the mass-7 abundance. This is described in Sec. IV.

IV. NARROW RESONANCE SOLUTION SPACE

In order to study the effect of resonances in different compound nuclei on the abundance of mass 7, our strategy is to specify the reaction rate for possible resonances, and then run the BBN code to find the mass-7 abundance in the presence of these resonances. In particular, for reactions involving light projectile X, we are interested in considering the general effect of states $^7A + X \rightarrow C^*$, including those associated with known energy levels in the compound nucleus, as well as possible overlooked states.

We assume that the narrow resonance approximation holds true at least as a rough guide. If the reaction pathway is specified, i.e., all of the nuclei $^7A + X \rightarrow C^* \rightarrow Y + Z$ are identified, then the reduced mass μ, reverse ratio and the Q-value are uniquely determined. In this case, the thermally averaged cross section is given by Eq. (13), with two free parameters: the product $\omega\Gamma_{\rm eff}$ and the resonance energy $E_{\rm res}$. Because the state C^* is unspecified, so is its spin J_*. On the other hand, we do know the spins of the initial state particles, and thus ω is specified up to a factor $2J_* + 1$ [Eq. (10)]. For this reason, the $\omega\Gamma_{\rm eff}$ dependence reduces to $(2J_* + 1)\Gamma_{\rm eff}$, which we explicitly indicate in all of our plots.

In a few cases we will be interested in one specific final quantum state, e.g., ^{7}Be(t, ^{3}He)^{7}Li; when the final state is specified, the reaction can be completely determined, including the effect of the reverse rates. However, in most situations we are interested in the possibility of an overlooked excited state in the compound nucleus, and thus in unknown final states. In this scenario we thus have only a ''generic'' inelastic exit channel. Consequently, for such plots we cannot evaluate the reverse reaction rate (which is in all interesting cases small) and so we set the reverse ratio to zero.

The resonant rates are included in the BBN code, individually for compound nuclei with an interesting initial state. The plots below show contours of constant, reduced mass-7 abundances. A general feature of all the plots is the near linear relation between $\log\Gamma_{\rm eff}$ and $E_{\rm res}$ in the region of larger, positive values of $\Gamma_{\rm eff}$ and $E_{\rm res}$. This can seen quantitatively as follows. The thermal rate is integrated

TABLE VI. As in Table I, listing the ground and excited final-state channels for the 18.43 MeV energy level in ^{10}B for the ^{7}Li + ^{3}He initial state.

Compound nucleus, J^{π}, E_{ex}	Initial state	L_{init}	L_{fin}	E_{res}	Γ_{tot}	Exit channels	Exit channel width
^{10}B,	^{7}Li + ^{3}He	0	unknown	641.7 keV	340 keV	γ(ground state)	$\geq$ 3 eV
2^{-}, 18.43 MeV			unknown			γ (4.77 MeV)	$\geq$ 17 eV
			0			$n + {}^{9}$B	unknown
			unknown			$n + {}^{9}$B* (1.6 MeV)	unknown
			0			$n + {}^{9}$B* (2.361 MeV)	unknown
			2			$n + {}^{9}$B* (2.75 MeV)	unknown
			1			$n + {}^{9}$B* (2.788 MeV)	unknown
			unknown			$n + {}^{9}$B* (4.3 MeV)	unknown
			2			$n + {}^{9}$B* (6.97 MeV)	unknown
			0			$p + {}^{9}$Be	unknown
			1			$p + {}^{9}$Be* (1.684 MeV)	unknown
			0			$p + {}^{9}$Be* (2.4294 MeV)	unknown
			2			$p + {}^{9}$Be* (2.78 MeV)	unknown
			1			$p + {}^{9}$Be* (3.049 MeV)	unknown
			1			$p + {}^{9}$Be* (4.704 MeV)	unknown
			0			$p + {}^{9}$Be* (5.59 MeV)	unknown
			2			$p + {}^{9}$Be* (6.38 MeV)	unknown
			3			$p + {}^{9}$Be* (6.76 MeV)	unknown
			0			$p + {}^{9}$Be* (7.94 MeV)	unknown
			2			$p + {}^{9}$Be* (11.283 MeV)	unknown
			0			$p + {}^{9}$Be* (11.81 MeV)	unknown
			1			$d + {}^{8}$Be	unknown
			1			$d + {}^{8}$Be* (3.03 MeV)	unknown
			1			$d + {}^{8}$Be* (11.35 MeV)	unknown
			1			$\alpha + {}^{6}$Li	unknown
			1			$\alpha + {}^{6}$Li* (2.186 MeV)	unknown
			1			$d + {}^{8}$Be* (4.31 MeV)	unknown
			1			$\alpha + {}^{6}$Li* (5.37 MeV)	unknown
			1			$\alpha + {}^{6}$Li* (5.65 MeV)	unknown
			0			^{3}He (elastic)	unknown

over time or equivalently temperature to give the final abundance of mass 7 or ^{7}Li as it exists. Now assuming that the thermal rate operates at an effective temperature T_{Li}, at which ^{7}Li production peaks, a given value for this effective $\langle\sigma v\rangle$ will give a fixed abundance. This implies

$$\delta Y_7/Y_7 \sim \langle\sigma v\rangle_{peak} \sim \Gamma_{eff} e^{-E_{res}/T_{Li}} \sim \text{constant}. \quad (15)$$

This gives a feel for the linear relation in the plot.

A. $A = 8$ compound nucleus

As seen in Table I, the only resonance energy level of interest in the ^{8}Li compound nucleus at 2.255 MeV is already accounted for in the ^{7}Li + n reaction. In the ^{8}Be compound nucleus, there are six levels of relevance for destroying either ^{7}Li or ^{7}Be at 16.922, 17.64, 18.91, 19.07, 19.24, and 19.40 MeV within our limit on E_{res}. The 16.922 MeV level is more than 300 keV below threshold and has a maximum total width of only 74 keV. Therefore, it is expected to have a weak effect. The 17.64 MeV level has typically low photon widths ($\approx$ 20 eV) and a total width of 10.7 keV. But this state's decay is dominated by the elastic channel which makes this channel uninteresting.

The energy level diagram for ^{8}Be [31] shows the initial state ^{7}Be + n at an entrance energy of E = 18.8997 MeV bringing the 18.91, 19.07, 19.235, and 19.40 MeV levels into play. From among these the effect of the 18.91, 19.07, and 19.235 MeV resonances are already accounted for in the well-known ^{7}Be$(n, p)^{7}$Li reaction [19]. The (18.91 MeV, 2^{-}) resonance with $L_{init} = 0$ is the dominant contributor [32,33]. Being a broad resonance with a total width of $\approx$ 122 keV, the Breit-Wigner form is not used and instead an R-matrix fit to the data [19] is used to evaluate the contribution of the resonant rate. The remaining level at 19.40 should also contribute to this reaction through ground and excited states. Only the 19.40 MeV channel can have an α exit channel due to parity considerations. And this resonance, despite a high resonance energy of $\approx$ 500 keV, can in principle be important due to its large total width of 645 keV, if the proton branching ratio is high.

TABLE VII. As in Table I, listing the ground and excited final-state channels for the 18.43 MeV energy level in ^{10}B for the ^{7}Be + t initial state.

Compound nucleus, J^π, E_{ex}	Initial state	L_{init}	L_{fin}	E_{res}	Γ_{tot}	Exit channels	Exit channel width
^{10}B,	^{7}Be + t	0	unknown	−239.1 keV	340 keV	γ(ground state)	$\geq$ 3 eV
2^-, 18.43 MeV			unknown			γ (4.77 MeV)	$\geq$ 17 eV
			0			n + ^{9}B	unknown
			unknown			n + ^{9}B* (1.6 MeV)	unknown
			0			n + ^{9}B* (2.361 MeV)	unknown
			2			n + ^{9}B* (2.75 MeV)	unknown
			1			n + ^{9}B* (2.788 MeV)	unknown
			unknown			n + ^{9}B* (4.3 MeV)	unknown
			2			n + ^{9}B* (6.97 MeV)	unknown
			0			p + ^{9}Be	unknown
			1			p + ^{9}Be* (1.684 MeV)	unknown
			0			n + ^{9}B* (2.4294 MeV)	unknown
			2			p + ^{9}Be* (2.78 MeV)	unknown
			1			p + ^{9}Be* (3.049 MeV)	unknown
			1			p + ^{9}Be* (4.704 MeV)	unknown
			0			p + ^{9}Be* (5.59 MeV)	unknown
			2			p + ^{9}Be* (6.38 MeV)	unknown
			3			p + ^{9}Be* (6.76 MeV)	unknown
			0			p + ^{9}Be* (7.94 MeV)	unknown
			2			p + ^{9}Be* (11.283 MeV)	unknown
			0			p + ^{9}Be* (11.81 MeV)	unknown
			1			d + ^{8}Be	unknown
			1			d + ^{8}Be* (3.03 MeV)	unknown
			1			d + ^{8}Be* (11.35 MeV)	unknown
			1			α + ^{6}Li	unknown
			1			α + ^{6}Li* (2.186 MeV)	unknown
			1			α + ^{6}Li* (4.31 MeV)	unknown
			1			α + ^{6}Li* (5.37 MeV)	unknown
			1			α + ^{6}Li* (5.65 MeV)	unknown
			0			t (elastic)	unknown

Figure 1 shows the ^{7}Li abundance in the (Γ_{eff}, E_{res}) plane for the ^{7}Be(n, p)^{7}Li reaction. Contours for ^{7}Li/$H \times 10^{10} = 1.23$, 2.0, 3.0, 4.0, and 5.0 (as labeled) are plotted as functions of the effective width and resonant energy. Below $\approx (2J_* + 1)40 = 120$ keV, we expect our results, based on the narrow resonance approximation, to be quite accurate. As one can see from this figure, to bring the ^{7}Li abundance down close to observed values, one would require a very low resonance energy (of order $\pm$30 keV) with a relatively large effective width. Unfortunately, the 19.40 MeV level of ^{8}Be corresponds to $E_{res} = 500$ keV as shown by the vertical dashed line and does not make any real impact on the ^{7}Li abundance.

Figure 2 shows the effect of a ^{8}B resonance with ^{7}Be and p in the initial state, plotted in the (Γ_{eff}, E_{res}) plane with contours of constant mass-7 abundances. According to Fig. 2 for resonance energies of a few tens of keV, resonance strength of a few meV is sufficient to attain the observational value of mass 7. However, from the energy level diagram for ^{8}B [34], the closest resonant energy level, E_{ex} is at 0.7695 MeV [34], whose effect is already included via the ^{7}Be(p, γ)^{8}B reaction. The experimental value of resonance energy is 632 keV which is off the scale in this figure. The only other close energy level to the ^{7}Be + p entrance channel is at −0.1375 MeV which means that the ground state is a subthreshold state. This is not the usual resonant reaction, since the ground state does not have a width in the sense we refer to a width for the other reactions. But at these energies, the astrophysical S-factor is $\approx$ 10 eV-barn which is very small and will yield a low cross section. This too is off scale in the figure and verifies that the ^{7}Be(p, γ)^{8}B reaction does not yield an important destruction channel.

B. $A = 9$ compound nucleus

The energy level diagram for ^{9}Be, [35] shows energy levels of interest at 16.671, 16.9752, and 17.298 MeV; these appear in Table II. The ^{7}Li + d entrance channel sits at 16.6959 MeV. The lowest lying resonant state is at 16.671 MeV and is a subthreshold state with $E_{res} = -24.9$ keV which lies within the total width of 41 keV.

TABLE VIII. As in Table I, listing the ground and excited final-state channels for the 18.80 MeV energy level in ^{10}B for the ^{7}Be + t initial state.

Compound nucleus, J^π, E_{ex}	Initial state	L_{init}	L_{fin}	E_{res}	Γ_{tot}	Exit channels	Exit channel width
^{10}B,	^{7}Be + t	1	unknown	130.9 keV	<600 keV	γ (0.72 MeV)	$\geq$ 20 eV
2^+, 18.80 MeV			unknown			γ (3.59 MeV)	$\geq$ 20 eV
			1			$n + {}^9$B	unknown
			unknown			$n + {}^9$B* (1.6 MeV)	unknown
			1			$n + {}^9$B* (2.361 MeV)	unknown
			1			$n + {}^9$B* (2.75 MeV)	unknown
			0			$n + {}^9$B* (2.788 MeV)	unknown
			unknown			$n + {}^9$B* (4.3 MeV)	unknown
			1			$n + {}^9$B* (6.97 MeV)	unknown
			1			$p + {}^9$Be	unknown
			2			$p + {}^9$Be* (1.684 MeV)	unknown
			1			$p + {}^9$Be* (2.4294 MeV)	unknown
			1			$p + {}^9$Be* (2.78 MeV)	unknown
			0			$p + {}^9$Be* (3.049 MeV)	unknown
			0			$p + {}^9$Be* (4.704 MeV)	unknown
			1			$p + {}^9$Be* (5.59 MeV)	unknown
			1			$p + {}^9$Be* (6.38 MeV)	unknown
			2			$p + {}^9$Be* (6.76 MeV)	unknown
			1			$p + {}^9$Be* (7.94 MeV)	unknown
			1			$p + {}^9$Be* (11.283 MeV)	unknown
			1			$p + {}^9$Be* (11.81 MeV)	unknown
			2			$d + {}^8$Be	unknown
			0			$d + {}^8$Be* (3.03 MeV)	unknown
			2			$d + {}^8$Be* (11.35 MeV)	unknown
			1			^{3}He + ^{7}Li	unknown
			1			^{3}He + ^{7}Li*(0.47761 MeV)	unknown
			2			$\alpha + {}^6$Li	unknown
			2			$\alpha + {}^6$Li* (2.186 MeV)	unknown
			2			$\alpha + {}^6$Li* (3.56 MeV)	unknown
			0			$\alpha + {}^6$Li* (4.31 MeV)	unknown
			0			$\alpha + {}^6$Li* (5.37 MeV)	unknown
			2			$\alpha + {}^6$Li* (5.65 MeV)	unknown
			1			t (elastic)	unknown

This resonance is thus obviously tantalizing—it is well-tuned energetically and involves an abundant, stable projectile. The ^{7}Li abundance contours for the ^{9}Be resonance states are shown in Fig. 3. Perhaps disappointingly, the figure shows that the effect on primordial mass 7 is minor. This illustrates the inability of direct ^{7}Li destruction channels to reduce the mass-7 abundance, as explained in Sec. II. Given the overall difficulty of this channel, it is clear that the other possible resonant energy levels (16.9752 MeV and 17.298 MeV) also fail to substantially reduce the mass-7 abundance.

The ^{9}B compound nucleus is relevant for studying the effect of the ^{7}Be$(d, p)2\alpha$ and its competitors such as ^{7}Be$(d, ^3$He$)^6$Li and ^{7}Be$(d, \alpha)^5$Li. As seen in Table III, the only two levels of interest here are the 16.71 and 17.076 MeV levels. The 16.71 MeV level corresponds to a resonance energy of 220 keV as shown by the vertical dashed line in Fig. 4 [36]. The widths are unknown experimentally. The approximate narrow resonance limit on the resonance width which is shown by the horizontal solid line is around 40 keV. The p exit channel leads to the ^{7}Be$(d, p)^8$Be* reaction through the excited state at 16.63 MeV in ^{8}Be. This should eventually lead to formation of alpha particles. Figure 4 shows the effect of the 16.71 MeV resonance on the mass-7 abundance as a function of the resonance strength and energy under the narrow resonance approximation. From the plot, we see that the ^{7}Li abundance is reduced by 50% for $(2J + 1)\Gamma_{\rm eff} = 240$ keV. This state has $J = 5/2$ and therefore, a value $\Gamma_{\rm eff} = 40$ keV or more will have substantial impact on the problem. Furthermore, as $\Gamma_L \geq \Gamma_{\rm eff}$, we require $\Gamma_L \gtrsim 40$ keV. This result confirms the conclusion of [16]. Later in Sec. V we will see how this compares with theoretical limits. As the decay widths are largely unknown, experimental data on the width are needed.

TABLE IX. As in Table I, listing the ground and excited final-state channels for the 19.29 MeV energy level in ^{10}B for the ^{7}Be + t initial state.

Compound nucleus, J^{π}, E_{ex}	Initial state	L_{init}	L_{fin}	E_{res}	Γ_{tot}	Exit channels	Exit channel width
^{10}B, 2^{-}, 19.29 MeV	^{7}Be + t	0	unknown	620.9 keV	190 ± 20 keV	γ	unknown
			0			$n + {}^{9}$B	unknown
			unknown			$n + {}^{9}$B* (1.6 MeV)	unknown
			0			$n + {}^{9}$B* (2.361 MeV)	unknown
			2			$n + {}^{9}$B* (2.75 MeV)	unknown
			1			$n + {}^{9}$B* (2.788 MeV)	unknown
			unknown			$n + {}^{9}$B* (4.3 MeV)	unknown
			0			$p + {}^{9}$Be	unknown
			1			$p + {}^{9}$Be* (1.684 MeV)	unknown
			0			$p + {}^{9}$Be* (2.4294 MeV)	unknown
			2			$p + {}^{9}$Be* (2.78 MeV)	unknown
			1			$p + {}^{9}$Be* (3.049 MeV)	unknown
			1			$p + {}^{9}$Be* (4.704 MeV)	unknown
			0			$p + {}^{9}$Be* (5.59 MeV)	unknown
			2			$p + {}^{9}$Be* (6.38 MeV)	unknown
			3			$p + {}^{9}$Be* (6.76 MeV)	unknown
			0			$p + {}^{9}$Be* (7.94 MeV)	unknown
			2			$p + {}^{9}$Be* (11.283 MeV)	unknown
			0			$p + {}^{9}$Be* (11.81 MeV)	unknown
			1			$d + {}^{8}$Be	unknown
			1			$d + {}^{8}$Be* (3.03 MeV)	unknown
			3			$d + {}^{8}$Be* (11.35 MeV)	unknown
			0			^{3}He	unknown
			1			$\alpha + {}^{6}$Li	unknown
			1			$\alpha + {}^{6}$Li* (2.186 MeV)	unknown
			1			$\alpha + {}^{6}$Li* (4.31 MeV)	unknown
			1			$\alpha + {}^{6}$Li* (5.37 MeV)	unknown
			1			$\alpha + {}^{6}$Li* (5.65 MeV)	unknown
			0			t (elastic)	unknown

The state at 17.076 MeV corresponds to a resonant energy of $E_{res} = 586$ keV and is beyond the scale shown in Fig. 4. A solution using this state is very unlikely.

C. $A = 10$ compound nucleus

Table IV shows that the ^{10}Be compound nucleus has energy levels at 17.12 and 17.79 MeV [37] which are close to the initial state ^{7}Li + t at 17.2509 MeV. The former is far below threshold and does not contribute to ^{7}Li destruction. The 17.79 MeV level is around 540 keV above the entrance energy and its spin and parity are unknown. The total width [37] is $\Gamma_{tot} = 112$ keV which implies a small overlap with the entry channel which renders this resonance insignificant despite having a number of n exit channels with both ground state and excited states of ^{9}Be. As seen in Fig. 5, the effect of ^{7}Li + t is small for the interesting region of parameter space.

The ^{10}B compound nucleus has energy levels at 18.2, 18.43, 18.80, and 19.29 MeV, which we investigate. The 18.2 MeV level is uncertain experimentally [38] as indicated in Table V, and hence ideal for parametrizing. There is a ^{3}He entrance channel a little over 400 keV below this level. The current total experimental width is 1.5 MeV which is very large and the branching ratios are unknown. The current uncertainty in the E_{res} is 200 keV. However, according to the plot in Fig. 5, even a 200 keV reduction in E_{res} would not be sufficient to cause any appreciable destruction of ^{7}Li as this reaction has negligible effect on the mass-7 abundance. This is another illustration of the fact that reactions involving direct destruction of ^{7}Li are unimportant.

The 18.43 MeV level is better understood [39] and with a resonance energy of ~640 keV for the ^{7}Li + ^{3}He initial state (Table VI) and a total width of 340 keV has a lower entrance probability and therefore is likely to be ineffective. This is evident from Fig. 5. This level is also a subthreshold resonance for the ^{7}Be + t state (Table VII), with resonance energy, $E_{res} = -239.1$ keV. This is far below threshold rendering it ineffective.

Staying with ^{7}Be + t, the closest energy level above the entrance energy of 18.669 MeV is the 18.80 MeV (2^{+}) level (Table VIII), which corresponds to a resonance energy of ≈ 130 keV [38]. The exit channel widths for p and ^{3}He are unknown experimentally and thus, this is a candidate for parametrization. There is a weak upper limit on $\Gamma_{tot} < 600$ keV [38], which for $J_{*} = 2$ is off scale in

TABLE X. As in Table I, listing resonances in ^{10}C, ^{11}B and ^{11}C.

Compound nucleus, J^π, E_{ex}	Initial state	L_{init}	L_{fin}	E_{res}	Γ_{tot}	Exit channels	Exit channel width
^{10}C, unknown	^{7}Be + ^{3}He	unknown	unknown unknown	unknown (Q = 15.003 MeV)	unknown	p α ^{3}He (elastic)	unknown unknown unknown
^{11}B, (3/2$^-$), 8.56 MeV	^{7}Li + α	0	1 1 1 1 1	−103.7 keV	1.346 eV	γ (ground state) γ (2.125 MeV) γ (4.445 MeV) γ (5.020 MeV) α (elastic)	0.53 ± 0.05 eV 0.28 ± 0.03 eV (4.7 ± 1.1) × 10^{-2} eV (8.5 ± 1.2) × 10^{-2} eV unknown
^{11}B, (5/2$^-$), 8.92 MeV (included)	^{7}Li + α	2	1 2 1 1	256.3 keV	4.37 ± 0.02 eV	γ (ground state) γ (ground state) γ (4.445 MeV) α (elastic)	4.10 ± 0.20 eV (5.0 ± 3.6) × 10^{-2} eV 0.22 ± 0.02 eV unknown
^{11}B, 7/2$^+$, 9.19 MeV	^{7}Li + α	3	1 2 0 1	526.3 keV	$1.9^{+1.5}_{-1.1}$ eV	γ (ground state) γ (4.445 MeV) γ (6.743 MeV) α (elastic)	(2.7 ± 1.2) × 10^{-9} eV 0.25 ± 0.09 eV (3.8 ± 1.3) × 10^{-2} eV unknown
^{11}B, 5/2$^+$, 9.271 MeV	^{7}Li + α	1	1 0 0 1 1	606.3 keV	4 keV	γ (ground state) γ (4.445 MeV) γ (6.743 MeV) γ (6.792 MeV) α (elastic)	0.212 eV 0.802 eV 0.137 eV <0.007 eV ≈ 4 keV
^{11}C, 3/2$^+$, 7.4997 MeV	^{7}Be + α	1	1 0 1	−43.3 keV	0.0105 eV	γ (ground state) γ (2.0 MeV) α (elastic)	unknown unknown unknown
^{11}C, (3/2$^-$), 8.10 MeV	^{7}Be + α	0	1 1 0	557 keV	11 ± 7 eV	γ (ground state) γ (2.0 MeV) α (elastic)	0.26 ± 0.06 eV (9.1 ± 2.3) × 10^{-2} eV unknown

Figs. 6 and 7. The contour plot in Fig. 6 shows that for a central value of resonance energy of ≈ 130 keV shown by the vertical dashed line, resonance strength of just under 1 MeV is required which is very high. Also, parity requirements force $L = 1$, which will cause suppression of this channel. We note that there is no quoted uncertainty for this energy level and neighboring levels have typical uncertainties of 100–200 keV. Therefore it may be possible (within 1–2σ) that the state lies at an energy of 100 keV lower and would energetically, have a chance at solving the ^{7}Li problem. This is true for the p exit channel.

The ^{3}He exit channel may also reduce mass 7, through the formation of the ^{7}Li which is much easier to destroy. This is reflected in Fig. 7, which shows that at resonance energies of ≤ 100 keV, a strength of a few 100 keV but less than 600 keV may be sufficient to achieve comparable destruction of ^{7}Be as the 16.71 MeV resonance. The caveat is that for such strength values, the narrow resonance approximation does not hold true and this may lead to a reduced effect. Nevertheless, this is yet another case deserving a detailed comparison with the theoretical limits which will follow in Sec. V. Once again, definitive conclusions can be drawn only based on experimental data.

The 19.29 MeV level (Table IX) is energetically harder to access and, with a total width of only 190 keV, it is unlikely to be of significance, despite being less studied.

The ^{10}C nucleus [40] appearing in Table X shows large uncertainties and experimental gaps at higher energy levels which may be relevant to entrance channels involving ^{7}Be. Reactions involving the ^{7}Be + ^{3}He initial state could contribute in destroying ^{7}Be if there exists a resonance in the parameter space shown in the Fig. 8. These reactions win over those involving the ^{7}Be + t state, because ^{3}He is substantially more abundant than t, but are worse off due to a higher Coulomb barrier. The entrance energy for ^{7}Be + ^{3}He is 15.0 MeV. As one can see from the figure, a 1$^-$ or 2$^-$ state with a resonance energy of either −10 keV or 40 keV corresponding to energy levels of 14.99 and 15.04 MeV, respectively, with a strength as high as a few tens of keVs is what it will take to solve the lithium

TABLE XI. This table lists surviving candidate resonances.

Compound nucleus, J^π, E_{ex}	Initial state	L_{init}	L_{fin}	E_{res}	Γ_{tot}	Exit channels	Exit channel width
^{9}B, ($5/2^+$), 16.71 MeV	^{7}Be + d	1	0	219.9 keV	unknown	$p + {}^8$Be* (16.63 MeV)	unknown
			1			$\alpha + {}^5$Li	unknown
^{10}B,	^{7}Be + t	1	1	130.9 keV	<600 keV	$p + {}^9$Be* (11.81 MeV)	unknown
2^+, 18.80 MeV			1			^{3}He	unknown
			2			α	unknown
^{10}C,	^{7}Be + ^{3}He unknown		unknown	unknown	unknown	p	unknown
unknown			unknown ($Q = 15.003$ MeV)			α	unknown
						^{3}He (elastic)	unknown

problem with this initial state. Thus, any ^{10}C resonance near these energies which may have been missed by experiment may be interesting as a solution to the lithium problem; we return to this issue in more detail in Sec. V.

D. $A = 11$ compound nucleus

For ^{11}B [41], Table X shows that the entrance channel ^{7}Li + α is at 8.6637 MeV which is 103.7 keV above the resonant energy level at 8.560 MeV and $\approx$ 260 keV below the resonant energy level at 8.92 MeV. Parity demands angular momentum to be 0. Both states are at relatively large $|E_{res}|$ and are not capable of making a sizable impact on the ^{7}Li abundance. Table X further lists states 9.19 MeV (which requires $L = 3$ and has a total width of <2 eV) and 9.271 MeV (whose decay is dominated by the elastic channel) which have progressively larger resonant energies and are unlikely to provide a solution.

For ^{11}C [42], the entrance channel, ^{7}Be + α is at 7.543 MeV which is 43 keV above the resonant energy level at 8.560 MeV and 557 keV below the resonant energy level at 8.10 MeV.

As seen in Fig. 9, we find that the subthreshold resonance in the ^{11}C nucleus produces a very insignificant effect on ^{7}Be in agreement with the claim in [16]. The superthreshold resonance states are also too far away at resonance energies, 557 keV and 260 keV for ^{7}Be(α, γ)^{11}C and ^{7}Li(α, γ)^{11}B, respectively.

However, Fig. 9 shows that the presence of a (missed) resonance at resonance energies of few tens of keV

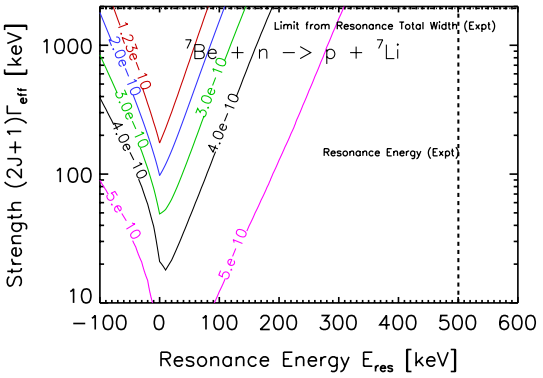

FIG. 1 (color online). The effect of resonances in the ^{8}Be compound nucleus involving initial states ^{7}Be + n. It shows the range of values for the product of the resonant state spin degeneracy and resonance strength $(2J + 1)\Gamma_{eff}$ versus the resonance energy. Contours indicate where the lithium abundance is reduced to $^7\text{Li}/H = 1.23 \times 10^{-10}$, 2.0×10^{-10}, 3.0×10^{-10}, 4.0×10^{-10}, and 5.0×10^{-10}. Normal resonances have $E_{res} > 0$, while subthreshold resonances lie in the $E_{res} < 0$. The horizontal dot-dashed line is the experimental value of the strength of the resonance corresponding to the 19.40 MeV energy level. The vertical dashed line shows the position of E_{res} for the same state.

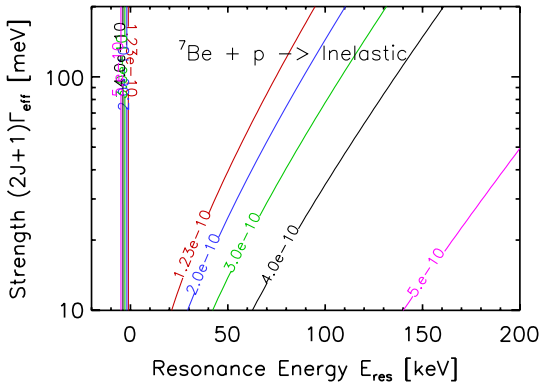

FIG. 2 (color online). As in Fig. 1, for the resonances in the ^{8}B compound nucleus involving initial states ^{7}Be + p.

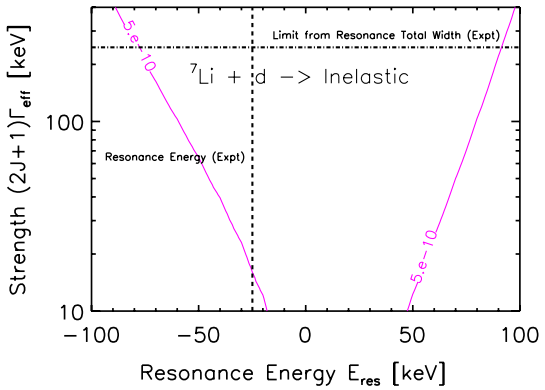

FIG. 3 (color online). As in Fig. 1, for the resonances in the ^{9}Be compound nucleus.

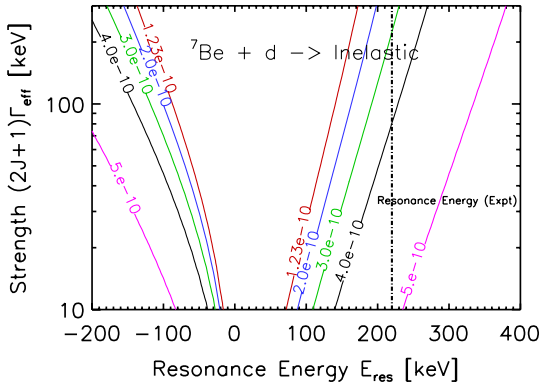

FIG. 4 (color online). As in Fig. 1, for the resonances in the ^{9}B compound nucleus. The vertical dashed line at 220 keV indicates the experimental central value of the resonance energy of the 16.71 MeV level.

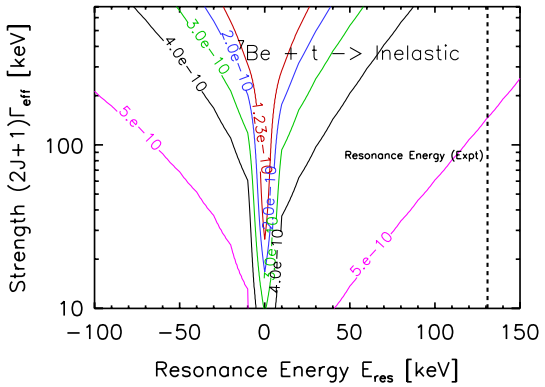

FIG. 6 (color online). As in Fig. 1, for the resonances in the ^{10}B compound nucleus involving initial states ^{7}Be + t.

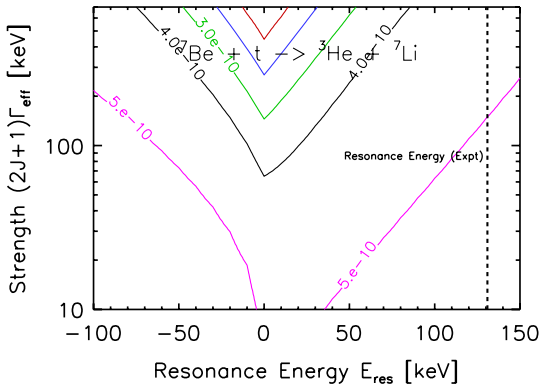

FIG. 7 (color online). As in Fig. 1, for the resonances in the reaction ^{7}Be(t, ^{3}He)^{7}Li.

requires a very meagre strength of the order of tens of meV to destroy mass 7 substantially. Strengths of this order are typical of electromagnetic channels. It is difficult to assess the probability that a ^{11}C state at 7.55 MeV has been overlooked.

V. REDUCED LIST OF CANDIDATE RESONANCES

Having systematically identified all possible known resonant energy levels which could affect BBN, we find most of these levels are ruled out immediately as promising solutions, based on their measured locations, strengths, and widths. As expected, the existing electromagnetic channels are too weak to cause significant depletion of lithium owing to their small widths.

From among the various hadronic channels listed in the tables, we have seen that all channels are unimportant except three, which are summarized in Table XI. The ^{7}Be + d channels involving the 16.71 MeV resonance in ^{9}B, the ^{7}Be + t channels involving the 18.80 MeV resonance in ^{10}B, and ^{7}Be + ^{3}He channels. These are ones where a more detailed theoretical calculation of widths is required to decide whether they may be important or not. For each reaction, the Wigner limit, Eq. (12), to the reduced width γ^2 imposes a bound on Γ_L via Eq. (11). Specifically, the penetration factor $P_L(E, a)$ must be estimated to see if the required strengths (according to Figs. 4 and 6–8) to solve the problem are at all attainable. The penetration factor is given by

$$P_L(E, a) = \frac{1}{G_L^2(E, a) + F_L^2(E, a)}, \tag{16}$$

where $G_L(E, a)$ and $F_L(E, a)$ are Coulomb wave functions.

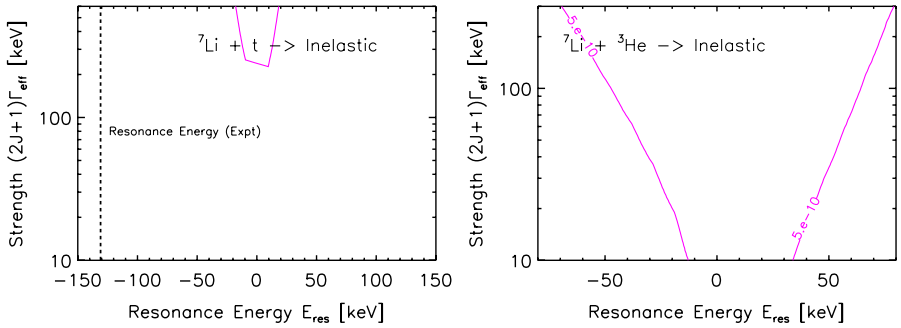

FIG. 5 (color online). As in Fig. 1, for the resonances in the ^{10}Be compound nucleus involving the initial state ^{7}Li + t (left), and in the ^{10}B compound nucleus involving the initial state ^{7}Li + ^{3}He. (right).

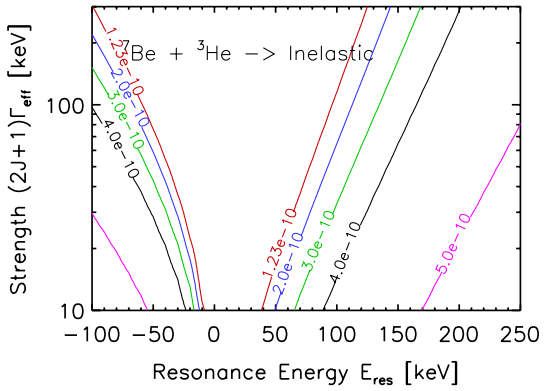

FIG. 8 (color online). As in Fig. 1, for the resonances in ^{10}C involving initial state ^{7}Be + ^{3}He.

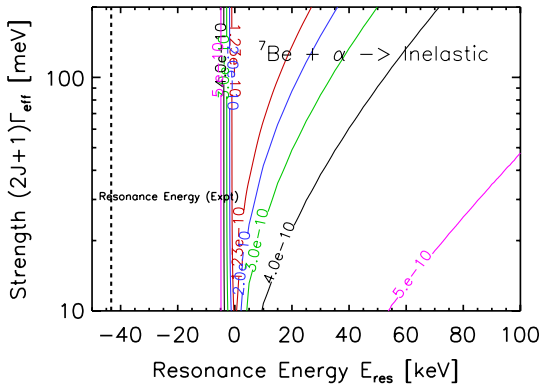

FIG. 9 (color online). As in Fig. 1, for the resonances in ^{11}C involving initial states ^{7}Be + α.

We note that the Coulomb barrier penetration factor decreases as the energy of the projectile and/or the channel radius a increases. For a narrow resonance, the relevant projectile energy is $E \approx E_{\rm res}$, which is set by nuclear experiments (where available) and their uncertainties. The channel radius corresponds to the boundary between the compound nucleus in the resonant state and the outgoing/incoming particles. Therefore, the channel radius depends on the properties of the compound state and the particles into which it decays.

Consider the case of ^{7}Be + d, which has resonance energy $E_{\rm res} = 220 \pm 100$ keV and initial angular momentum $L_{\rm init} = 1$. A naive choice for the channel radius is the "hard-sphere" approximation

$$a_{12} = 1.45(A_1^{1/3} + A_2^{1/3})\ \text{fm}, \tag{17}$$

which gives $a_{27} = 4.6$ fm. Using the Coulomb functions, Γ_1 is of order a few keV. The corresponding strength $\Gamma_{\rm eff}$ should be essentially the same and we further gain a factor of 6 from the spin of this state. This suggests, by using Fig. 4, that this resonance should fall short of the width required to solve or even ameliorate the problem.

However, reactions involving light nuclides including $A = 7$ are found to have channel radii exceeding the hard-sphere approximation [16]. We thus consider larger radii and find that for values higher than around 10 fm, we get a width which has the potential to change the ^{7}Li abundance noticeably. The Wigner limit

$$a^2 = \frac{3\hbar^2}{2\mu E_{\rm res}} \tag{18}$$

gives a larger radius, $a_{27} = 13.5$ fm, which gives one a better chance of solving the problem. This is consistent with the conclusions drawn by [16].

For the ^{7}Be + t initial state, the 18.80 MeV state of ^{10}B has a resonance energy $E = 0.131$ MeV and $L_{\rm init} = 1$. There is no experimental error bar on the resonance energy. The hard-sphere approximation gives $a_{37} = 4.9$ fm. This gives a width Γ_1 which is less than a tenth of a keV, and is orders of magnitude lower than what is needed. In the spirit of what we did in the earlier case, using Eq. (18) gives a channel radius, $a_{37} = 15$ fm improving the situation by almost 2 orders of magnitude in Γ_1. If, in addition to increasing a_{37}, the resonance energy were to be higher by 100 keV, then Γ_1 could be large enough to change the ^{7}Li abundance noticeably.

The ^{7}Be + ^{3}He initial state will have ^{10}C as the compound state. The structure of the ^{10}C nucleus is not well studied experimentally [40] nor theoretically. In particular, we are unaware of any published data on ^{10}C states near the ^{7}Be + ^{3}He entrance energy, i.e., states at or near $E_{\rm ex}(^{10}\text{C}) \approx Q(^7\text{Be} + {}^3\text{He}) = 15.003$ MeV. To our knowledge, there has not been any search for narrow states in this region. The potential exit channels of importance are ^{9}B + p and ^{6}Be + α. Because $J^\pi(^3\text{He}) = 1/2^+ J^\pi(^7\text{Be}) = 3/2^-$, to have $L_{\rm init} = 0$ and thus no entrance angular momentum barrier would require the ^{10}C state to have

$$J^\pi = (1 \quad \text{or} \quad 2)^-. \tag{19}$$

Because $J^\pi(^9\text{B}) = 3/2^-$, the entrance channel spin and parity required to give $L_{\rm init} = 0$ will also allow $L_{\rm fin} = 0$ for the ^{9}B + p. On the other hand, in the final-state ^{6}Be + α both ^{6}Be and ^{4}He have $J^\pi = 0^+$. Thus if the putative ^{10}C state has $J^\pi = 1^-$, this forces the ^{6}Be + α final state to have $L_{\rm fin} = 1$, and thus this channel will be suppressed by an angular momentum barrier relative to ^{9}B + p.

Using Eq. (17), we again get $a_{37} = 4.9$ fm. Taking $L_{\rm init} = 0$ and $E = 0.2$ MeV, Γ_0 is about 10^{-3} keV and is extremely small. However, the penetration factor is highly sensitive to the channel radius and a relatively small increase in a increases the width by orders of magnitude. Increasing the energy does reduce the penetration barrier, but a higher width is required due to thermal suppression. In order to get a sizable width, which is required to solve the problem according to Fig. 8, a_{37} must be $\gtrsim 30$ fm. At this energy, this radius is somewhat larger than what is afforded by Eq. (18).

VI. DISCUSSION AND CONCLUSIONS

The lithium problem was foreshadowed before precision cosmic microwave background data were cast in stark light by the first-year WMAP results, and has only worsened since. While astrophysical solutions are not ruled out, they are increasingly constrained. Thus, a serious and thorough evaluation of all possible nuclear physics aspects of primordial lithium production is urgent in order to determine whether the lithium problem truly points to new fundamental physics.

Reactions involving the primordial *production* of mass 7, and its lower-mass progenitor nuclides, are very well-studied experimentally and theoretically and leave no room for surprises at the level needed to solve the lithium problem [3,15,16]. Lithium *destruction* reactions are less well-determined. While the dominant destruction channels $^7\mathrm{Be}(n,p)^7\mathrm{Li}$ and $^7\mathrm{Li}(p,\alpha)\alpha$ have been extensively studied, in contrast, the subdominant destruction channels are less well-constrained.

We therefore have exhaustively cataloged possible resonant, mass-7 destruction channels. As evidenced by the large size of Tables I, II, III, IV, V, VI, VII, VIII, IX, and X, the number of potentially interesting compound states is quite large. However, it is evident that the basic conservation laws such as angular momentum and parity, coupled with the requirement of resonant reactions to be 2–3 times the $^7\mathrm{Be}(n,p)^7\mathrm{Li}$ rate, prove to be extremely restrictive on the options for a resonant solution to the lithium problem, and reduce the possibilities dramatically.

Given existing nuclear data, there are several choices for experimentally identified nuclear resonances which come close to removing the discrepancy between the lithium WMAP + BBN predictions and observations as tabulated in Sec. V. The 16.71 MeV level in ^{9}B compound nucleus and the 18.80 MeV level in the ^{10}B compound nucleus are two such candidates. It is possible, however, that resonant effects have been neglected in reactions passing through states which have been entirely missed. In all of the plots above, we have illustrated the needed positions and strengths of such states, if they exist. One possibility involving the compound state ^{10}C is poorly studied experimentally, especially at higher energy states close to the Q-value for $^7\mathrm{Be} + {}^3\mathrm{He}$.

Any of these resonances (or a combination) could offer a partial or complete solution to the lithium problem, but in each case, we find that large channel radii ($a > 10$ fm) are needed in order that the reaction widths are large enough. We confirm the results of Cyburt and Pospelov [16] in this regard concerning $^7\mathrm{Be} + d$, and we also find similar channel radii are needed for $^7\mathrm{Be} + t$, while larger radii are required for $^7\mathrm{Be} + {}^3\mathrm{He}$. Obviously, nature need not be so kind (or mischievous!) in providing such fortuitous fine-tuning. But given the alternative of new physics solutions to the lithium problem, it is important that all conventional approaches be exhausted.

Thus, based on our analysis, quantum mechanics could allow resonant properties that can remove or substantially reduce the lithium discrepancy. An experimental effort to measure the properties of these resonances, however, can conclusively rule out these resonances as solutions. If all possible resonances are measured and found to be unimportant for BBN, this together with other recent work [15] will remove any chance of a ''nuclear solution'' to the lithium problem and substantially increase the possibility of a new physics solution. Thus, regardless of the outcome, experimental probes of the states we have highlighted will complete the firm empirical foundation of the nuclear physics of BBN and will make a crucial contribution to our understanding of the early universe.

ACKNOWLEDGMENTS

We are pleased to acknowledge useful and stimulating conversations with Robert Wiringa, Livius Trache, Shalom Shlomo, Maxim Pospelov, Richard Cyburt, and Robert Charity. The work of K. A. O. was supported in part by DOE Grant No. DE-FG02-94ER-40823 at the University of Minnesota.

APPENDIX A: THE NARROW RESONANCE APPROXIMATION

Consider a reaction $A + b \rightarrow C^* \rightarrow c + D$, which passes through an excited state of the compound nucleus C^*. We treat separately normal and subthreshold reactions, defined, respectively, by a positive and negative sign of the resonance energy $E_{\mathrm{res}} = E_{\mathrm{ex}} - Q_C$, where E_{ex} is the excitation energy of the C^* state considered, and $Q_C = \Delta(A) + \Delta(B) - \Delta(C^*)$.

In general, the thermally averaged rate is

$$\langle \sigma v \rangle = \frac{\int d^3 v e^{-\mu v^2/2T} \sigma v}{\int d^3 v e^{-\mu v^2/2T}} = \sqrt{\frac{8}{\pi\mu}} T^{-3/2} \int_0^\infty dE E \sigma(E) e^{-E/T}. \quad \text{(A1)}$$

For a Breit-Wigner resonance with widths not strongly varying with energy, this becomes

$$\langle \sigma v \rangle = \frac{4\pi\omega\Gamma_{\mathrm{init}}\Gamma_{\mathrm{fin}}}{(2\pi\mu T)^{3/2}} \int_0^\infty dE \frac{e^{-E/T}}{(E - E_{\mathrm{res}})^2 + (\Gamma_{\mathrm{tot}}/2)^2}. \quad \text{(A2)}$$

Thus the thermal rate is controlled by the integral of the Lorentzian resonance profile modulated with the exponential Boltzmann factor.

The narrow resonance approximation has usually only been applied to the normal resonance case, and assumes that the total resonance width is small compared to the temperature, $\Gamma_{\mathrm{tot}} \ll T$.

1. Narrow normal resonances

In the normal or "superthreshold" case, the integral includes the peak of the Lorentzian where $E = E_{\rm res}$. The narrow condition then guarantees that over the Lorentzian width, the Boltzmann factor does not change appreciably, and so we make the approximation

$$\exp\left(-\frac{E}{T}\right) \approx \exp\left(-\frac{\hat{E}}{T}\right), \tag{A3}$$

where we choose the "typical" energy to be the peak of the Lorentzian, $\hat{E} = E_{\rm res}$. Then the integral becomes

$$\langle \sigma v \rangle_{\Gamma_{\rm tot} \ll T} \approx \frac{\omega \Gamma_{\rm init} \Gamma_{\rm fin}}{2(2\pi\mu T)^{3/2}} e^{-E_{\rm res}/T} \times \int_0^\infty dE \frac{1}{(E - E_{\rm res})^2 + (\Gamma_{\rm tot}/2)^2}. \tag{A4}$$

Furthermore, it is usually also implicitly assumed that the resonance energy is large compared to the width, $E_{\rm res} \gg \Gamma_{\rm tot}$. Then the integral gives $2\pi/\Gamma_{\rm tot}$, and the thermally averaged cross section under this approximation is given by [43]

$$\langle \sigma v \rangle_{\Gamma_{\rm tot} \ll T, E_{\rm res}} = \omega \Gamma_{\rm eff} \left(\frac{2\pi}{\mu T}\right)^{3/2} e^{-E_{\rm res}/T} \tag{A5}$$

$$= 2.65 \times 10^{-13} \mu^{-3/2} \omega \Gamma_{\rm eff} T_9^{-3/2} \times \exp(-11.605 E_{\rm res}/T_9) \ {\rm cm}^3 \ {\rm s}^{-1}, \tag{A6}$$

where the latter expression has $T_9 = T/10^9$ K.

Note, however, that Eq. (A2) is exactly integrable as it stands and does not require that we make the usual $E_{\rm res} \gg \Gamma_{\rm tot}$ approximation. Thus for the normal case we modify the usual reaction rate and instead adopt the form

$$\langle \sigma v \rangle_{\rm narrow, normal} = \langle \sigma v \rangle_{\Gamma_{\rm tot} \ll T, E_{\rm res}} f(2E_{\rm res}/\Gamma_{\rm tot}). \tag{A7}$$

Here we introduce a temperature-independent correction for finite $E_{\rm res}/\Gamma_{\rm tot}$ (still with $E_{\rm res} > 0$)

$$f(u) = \frac{1}{2} + \frac{1}{\pi} \arctan u. \tag{A8}$$

This factor spans $f \to 1/2$ for $E_{\rm res} \ll \Gamma_{\rm tot}$ to $f \to 1$ for $E_{\rm res} \gg \Gamma_{\rm tot}$.

In practice, we adopt a slightly modified version of the correction factor in our plots. Recall that in Figs. 2–9, we show results for lithium abundances in the presence of resonant reactions with fixed input channels, but without reference to a specific final state. Without the correction factor, the resonant reaction rate is characterized by two parameters, $E_{\rm res}$ and $\Gamma_{\rm eff}$. These two parameters are insufficient to specify the correction factor, which depends on $E_{\rm res}/\Gamma_{\rm tot}$. Rather than separately introduce $\Gamma_{\rm tot}$, we instead approximate the correction factor as $f(2E_{\rm res}/\Gamma_{\rm eff})$. Because $\Gamma_{\rm eff} < \Gamma_{\rm tot}$ and f is monotonically increasing, this always *underestimates* the value of f and thus conservatively *understates* the importance of the resonance we seek (but the approximation is never off by more than a factor of 2 in the normal case).

2. Narrow subthreshold resonances

Still making the narrow resonance approximation $\Gamma_{\rm tot} \ll T$, we now turn to the subthreshold case, in which $E_{\rm res} < 0$. To make the effect of the sign change explicit, we rewrite Eq. (A2) as

$$\langle \sigma v \rangle = \frac{\omega \Gamma_{\rm init} \Gamma_{\rm fin}}{2(2\pi\mu T)^{3/2}} \int_0^\infty dE \frac{e^{-E/T}}{(E + |E_{\rm res}|)^2 + (\Gamma_{\rm tot}/2)^2}. \tag{A9}$$

Now the integrand always excludes the resonant peak and only includes the high-energy wing. As with the normal case, the narrowness of the resonance implies that the Boltzmann exponential does not change much, where the Lorentzian has a significant contribution, and so we again will approximate $e^{-E/T} \approx e^{-\hat{E}/T}$. Since we avoid the resonant peak, the choice of $\hat{E}$ is not as straightforward in the subthreshold case where we took $\hat{E} = E_{\rm res}$. This choice makes no sense in the subthreshold case, because the $e^{-E_{\rm res}/T} > 1$ in the subthreshold case, yet obviously kinetic energy $E > 0$ and thus the Boltzmann factor must always be a suppression and not an enhancement!

Yet clearly $|E_{\rm res}|$ remains an important scale. Thus we put $\hat{E} = \hat{u}|E_{\rm res}|$, and we have examined results for different values of the dimensionless parameter $\hat{u}$. We find good agreement with numerical results when we adopt $\hat{u} \approx 1$, i.e., $\hat{E} = |E_{\rm res}|$. Thus for the subthreshold case we adopt a reaction rate which is closely analogous to the normal case,

$$\langle \sigma v \rangle_{\rm narrow, subthreshold} = \omega \Gamma_{\rm eff} \left(\frac{2\pi}{\mu T}\right)^{3/2} e^{-|E_{\rm res}|/T} f(-2|E_{\rm res}|/\Gamma_{\rm tot}). \tag{A10}$$

Similarly to the normal case, as the reaction becomes increasingly off-resonance, i.e., as $|E_{\rm res}|$ grows, there is an exponential suppression. In addition, the correction factor has limits $f \to 1/2$ for $|E_{\rm res}| \ll \Gamma_{\rm tot}$, and $f \to 0$ as $|E_{\rm res}| \gg \Gamma_{\rm tot}$. Finally, note that, as a function of $E_{\rm res}$, our subthreshold and normal rates match at $E_{\rm res} = 0$, as they must physically.

[1] R. H. Cyburt, B. D. Fields, and K. A. Olive, New Astron. Rev. **6**, 215 (2001).

[2] A. Coc, E. Vangioni-Flam, P. Descouvemont, A. Adahchour, and C. Angulo, Astrophys. J. **600**, 544 (2004).

[3] R. H. Cyburt, B. D. Fields, and K. A. Olive, Phys. Lett. B **567**, 227 (2003); A. Cuoco, F. Iocco, G. Mangano, G. Miele, O. Pisanti, and P. D. Serpico, Int. J. Mod. Phys. A **19**, 4431 (2004); B. D. Fields and S. Sarkar, Phys. Lett. B **667**, 1 (2008); P. Descouvemont, A. Adahchour, C. Angulo, A. Coc, and E. Vangioni-Flam, At. Data Nucl. Data Tables **88**, 203 (2004); G. Steigman, Annu. Rev. Nucl. Part. Sci. **57**, 463 (2007).

[4] R. H. Cyburt, Phys. Rev. D **70**, 023505 (2004).

[5] R. H. Cyburt, B. D. Fields, and K. A. Olive, J. Cosmol. Astropart. Phys. 11 (2008) 012.

[6] R. H. Cyburt, B. D. Fields, K. A. Olive, and E. Skillman, Astropart. Phys. **23**, 313 (2005).

[7] E. Komatsu *et al.*, Astrophys. J. Suppl. Ser. **192**, 18 (2011).

[8] F. Spite and M. Spite, Astron. Astrophys. **115**, 357 (1982).

[9] S. G. Ryan, T. C. Beers, K. A. Olive, B. D. Fields, and J. E. Norris, Astrophys. J. **530**, L57 (2000).

[10] P. Bonifacio *et al.*, Astron. Astrophys. **390**, 91 (2002); L. Pasquini and P. Molaro, Astron. Astrophys. **307**, 761 (1996); F. Thevenin, C. Charbonnel, J. A. de Freitas Pacheco, T. P. Idiart, G. Jasniewicz, P. de Laverny, and B. Plez, Astron. Astrophys. **373**, 905 (2001); P. Bonifacio, Astron. Astrophys. **395**, 515 (2002); K. Lind, F. Primas, C. Charbonnel, F. Grundahl, and M. Asplund, Astron. Astrophys. **503**, 545 (2009).

[11] J. I. G. Hernandez *et al.*, Astron. Astrophys. **505**, L13 (2009).

[12] S. Vauclair and C. Charbonnel, Astrophys. J. **502**, 372 (1998); M. H. Pinsonneault, T. P. Walker, G. Steigman, and V. K. Narayanan, Astrophys. J. **527**, 180 (1999); M. H. Pinsonneault, G. Steigman, T. P. Walker, and V. K. Narayanan, Astrophys. J. **574**, 398 (2002); O. Richard, G. Michaud, and J. Richer, Astrophys. J. **619**, 538 (2005); A. J. Korn *et al.*, Nature (London) **442**, 657 (2006).

[13] C. Angulo *et al.*, Astrophys. J. **630**, L105 (2005).

[14] R. H. Cyburt, B. D. Fields, and K. A. Olive, Phys. Rev. D **69**, 123519 (2004).

[15] R. N. Boyd, C. R. Brune, G. M. Fuller, and C. J. Smith, Phys. Rev. D **82**, 105005 (2010).

[16] R. H. Cyburt and M. Pospelov, arXiv:0906.4373.

[17] V. F. Dmitriev, V. V. Flambaum, and J. K. Webb, Phys. Rev. D **69**, 063506 (2004); A. Coc, N. J. Nunes, K. A. Olive, J. P. Uzan, and E. Vangioni, Phys. Rev. D **76**, 023511 (2007).

[18] K. Jedamzik, Phys. Rev. D **70**, 063524 (2004); J. L. Feng, S. Su, and F. Takayama, Phys. Rev. D **70**, 075019 (2004); J. R. Ellis, K. A. Olive, and E. Vangioni, Phys. Lett. B **619**, 30 (2005); K. Jedamzik, K. Y. Choi, L. Roszkowski, and R. Ruiz de Austri, J. Cosmol. Astropart. Phys. 07 (2006) 007; R. H. Cyburt, J. R. Ellis, B. D. Fields, K. A. Olive, and V. C. Spanos, J. Cosmol. Astropart. Phys. 11 (2006) 014; M. Pospelov, J. Pradler, and F. D. Steffen, J. Cosmol. Astropart. Phys. 11 (**2008**) 020; T. Jittoh, K. Kohri, M. Koike, J. Sato, T. Shimomura, and M. Yamanaka, Phys. Rev. D **78**, 055007 (2008); K. Jedamzik and M. Pospelov, New J. Phys. **11**, 105028 (2009); . R. H. Cyburt, J. Ellis, B. D. Fields, F. Luo, K. A. Olive, and V. C. Spanos, J. Cosmol. Astropart. Phys. 10 (2009) 021; 10 (2010) 032; M. Kusakabe, T. Kajino, R. N. Boyd, T. Yoshida, and G. J. Mathews, Phys. Rev. D **76**, 121302 (2007); M. Kusakabe, T. Kajino, R. N. Boyd, T. Yoshida, and G. J. Mathews, Astrophys. J. **680**, 846 (2008).

[19] R. H. Cyburt, Phys. Rev. D **70**, 023505 (2004).

[20] S. Ando, R. H. Cyburt, S. W. Hong, and C. H. Hyun, Phys. Rev. C **74**, 025809 (2006).

[21] R. H. Cyburt and B. Davids, Phys. Rev. C **78**, 064614 (2008).

[22] R. B. Wiringa, S. C. Pieper, J. Carlson, and V. R. Pandharipande, Phys. Rev. C **62**, 014001 (2000); S. C. Pieper, K. Varga, and R. B. Wiringa, Phys. Rev. C **66**, 044310 (2002).

[23] F. Hoyle, Astrophys. J. Suppl. Ser. **1**, 121 (1954).

[24] TUNL Nuclear Data Evaluation Group, Energy Levels of Light Nuclei, $A = 3 - 20$, http://www.tunl.duke.edu/nucldata/; D. R. Tilley, J. H. Kelley, J. L. Godwin, D. J. Millener, J. E. Purcell, C. G. Sheu, and H. R. Weller, Nucl. Phys. **A745**, 155 (2004); F. Ajzenberg-Selove, Nucl. Phys. **A506**, 1 (1990).

[25] R. Esmailzadeh, G. D. Starkman, and S. Dimopoulos, Astrophys. J. **378**, 504 (1991).

[26] V. F. Mukhanov, Int. J. Theor. Phys. **43**, 669 (2004).

[27] Information extracted from National Nuclear Data Center, "Chart of Nuclides," http://www.nndc.bnl.gov/chart/.

[28] R. V. Wagoner, W. A. Fowler, and F. Hoyle, Astrophys. J. **148**, 3 (1967).

[29] M. S. Smith, L. H. Kawano, and R. A. Malaney, Astrophys. J. Suppl. Ser. **85**, 219 (1993); L. M. Krauss and P. Romanelli, Astrophys. J. **358**, 47 (1990); G. Fiorentini, E. Lisi, S. Sarkar, and F. L. Villante, Phys. Rev. D **58**, 063506 (1998).

[30] T. Teichmann, and E. P. Wigner, Phys. Rev. **87**, 123 (1952).

[31] TUNL Nuclear Data Evaluation Project, "Energy Level Diagram, 8Be," http://www.tunl.duke.edu/nucldata/figures/08figs/08_04_2004.gif.

[32] A. Coc, E. Vangioni-Flam, P. Descouvemont, A. Adahchour, and C. Angulo, Astrophys. J. **600**, 544 (2004).

[33] A. Adahchour and P. Descouvemont, J. Phys. G **29**, 395 (2003).

[34] TUNL Nuclear Data Evaluation Project, "Energy Level Diagram, 8B," http://www.tunl.duke.edu/nucldata/figures/08figs/08_05_2004.gif.

[35] TUNL Nuclear Data Evaluation Project, "Energy Level Diagram, 9Be," http://www.tunl.duke.edu/nucldata/figures/09figs/09_04_2004.gif.

[36] TUNL Nuclear Data Evaluation Project, "Energy Level Diagram, 9B," http://www.tunl.duke.edu/nucldata/figures/09figs/09_05_2004.gif.

[37] TUNL Nuclear Data Evaluation Project, "Energy Level Diagram, 10Be," http://www.tunl.duke.edu/nucldata/figures/10figs/10_04_2004.gif.

[38] TUNL Nuclear Data Evaluation Project, "Energy Level Diagram, 10B," http://www.tunl.duke.edu/nucldata/figures/10figs/10_05_2004.gif.
[39] J. Yan, F. E. Cecil, U. Greife, C. C. Jewett, R. J. Peterson, and R. A. Ristenin, Phys. Rev. C **65**, 048801 (2002).
[40] TUNL Nuclear Data Evaluation Project, "Energy Level Diagram, 10C," http://www.tunl.duke.edu/nucldata/figures/10figs/10_06_2004.gif.
[41] TUNL Nuclear Data Evaluation Project, "Energy Level Diagram, 11B," http://www.tunl.duke.edu/nucldata/figures/11figs/11_05_1990.gif.
[42] TUNL Nuclear Data Evaluation Project, "Energy Level Diagram, 11C," http://www.tunl.duke.edu/nucldata/figures/11figs/11_06_1990.gif.
[43] C. Angulo *et al.*, Nucl. Phys. **A656**, 3 (1999).